Check for updates

In or Out of Equilibrium? How Microbial Activity Controls the Oxygen Isotopic Composition of Phosphate in Forest Organic Horizons With Low and High Phosphorus Availability

Chiara Pistocchi[1,2], Éva Mészáros[1,3], Emmanuel Frossard[1], E. K. Bünemann[1,4] and Federica Tamburini[1]*

[1] Institute of Agricultural Science, ETH Zürich, Zurich, Switzerland, [2] Eco&Sols, Montpellier SupAgro, Univ Montpellier, CIRAD, INRAE, IRD, Montpellier, France, [3] Department of Biosystems Science and Engineering, ETH Zürich, Basel, Switzerland, [4] Department of Soil Sciences, Research Institute of Organic Agriculture FiBL, Frick, Switzerland

While there are estimates of the abiotic processes contribution to soil phosphorus (P) availability, less is known about the contribution of biological processes. Two main enzymatic processes involved in soil P cycling are known to alter the oxygen isotopic composition of phosphate (δ^{18}O-P), each in a different way, through the cleavage of the P–O bond: the intracellular P turnover and the organic P hydrolysis. The former induces isotopic equilibration between phosphate and water and is considered the major process affecting soil available P via microbial P release. The latter induces depleted δ^{18}O-P in the phosphate released from the mineralization of organic P. We studied P dynamics in organic horizons of two contrasting soils (low- and high-P availability) from temperate beech forests. We labeled the soil with ^{18}O-enriched water and followed changes in the δ^{18}O-P of different soil P pools in the presence or absence of added leaf litter during 3 months of incubation. δ^{18}O-P values of almost all P pools progressively increased indicating oxygen incorporation from the enriched soil water into phosphate via the above-mentioned enzymatic processes. δ^{18}O-P of available P increased more in the P-rich soil than in the P-poor soil and approached the isotopic equilibrium between phosphate and water, revealing the impact of microbial P release into the available P pool. However, in the P-poor soil, the available P brought the isotopic signature induced by phosphatase enzymes, indicating that it was mostly originated from the hydrolysis of organic P. Therefore, under P-limiting conditions, the isotopic effect of organic P hydrolysis can outweigh the isotopic equilibrium effect. Finally, two independent isotopic approaches with ^{33}P and δ^{18}O-P provided very similar estimates of P exchanged between the available P and other inorganic soil pools. This suggests that δ^{18}O-P can be successfully used to trace P fluxes, provided that the underlying processes do not break the P–O bonds of the phosphate molecule.

Keywords: soil, isotopic labeling, phosphatase, microbial phosphorus, mineralization

INTRODUCTION

In forest ecosystems, plants and their mycorrhizae take up most of their phosphorus (P) as dissolved orthophosphate (PO_4^{3-}, hereafter phosphate) from the soil solution, which represents often a small proportion of the total P in soil. The soil solution is continuously replenished by abiotic processes, such as the release of P from sorbed phases, by the dissolution of P containing minerals, and by biological processes, namely mineralization of organic P (Po). Microbes mineralize Po from plant litter and soil organic matter via enzymatic hydrolysis. The newly released P is taken up by microbes (immobilization), sorbed to the soil solid phases or replenishes the soil solution. Upon cell death, microbial P ultimately enters the non-living Po and inorganic P pools, thus constituting a potentially available P pool.

While there are estimates of the contribution of abiotic inorganic P pools to P availability (Helfenstein et al., 2020), less is known about the contribution of biological processes. This contribution varies widely, depending on factors such as land-use and inorganic P availability (Becquer et al., 2014; Bünemann, 2015; Pistocchi et al., 2018). Integrating this knowledge into soil P cycling models is crucial to predict the effects of changing environmental conditions, such as the ones induced by climate change, or of global P resources scarcity on net primary production.

Assessing soil P dynamics is challenging, because exchanges between P pools often occur without net changes in pool size. The use of radioactive tracers ^{33}P and ^{32}P is to date the sole option to quantify gross P fluxes, such as gross P immobilization and mineralization (Bünemann, 2015 and references therein), the transfer from the soil to the plant (Frossard et al., 2011 and references therein) and the fate of P added with plant residues or fertilizers (Fardeau et al., 1995; Daroub et al., 2000; Pistocchi et al., 2018). Studies on various forest soils have highlighted the impact of Po mineralization on P fluxes notably when inorganic P availability is low (Achat et al., 2009; Mooshammer et al., 2012; Spohn et al., 2013; Bünemann et al., 2016; Pistocchi et al., 2018).

Although radioisotopes have several advantages (e.g., negligible P mass addition, direct P tracing, simple to analyze), they also have several drawbacks related to safety issues, short half-lives, and low sensitivity to biological P fluxes when the baseline of isotopic dilution, i.e., the flux due to abiotic processes, is high (Pistocchi et al., 2018; Siegenthaler et al., 2020).

In the last two decades, many studies have shown that biological processes involved in soil P cycling alter the isotopic composition of oxygen in phosphate (δ^{18}O-P) through the cleavage of the P–O bond and the incorporation of O atoms from water (Tamburini et al., 2012 and references therein). Whereas in the absence of biological activity, the P–O bond is stable and exchanges of oxygen (O) between phosphate and water are negligible. Two main enzyme-mediated processes have an impact on δ^{18}O-P. Firstly, intracellular P turnover controlled by the enzyme inorganic pyrophosphatase leads to the complete exchange of the four O atoms in phosphate with O from

water. This reaction produces a temperature-dependent isotopic equilibrium between phosphate and water (Longinelli and Nuti, 1973; Chang and Blake, 2015).

Secondly, the intra- and extracellular phosphatase enzymes incorporate one or two O atoms from water into phosphate released by the breakdown of Po compounds (P mono- and diesters). One O atom is incorporated during the hydrolysis of a phosphomonoester and two O atoms are incorporated during the hydrolysis of a phosphodiester. These transfers are associated with an enzyme-dependent fractionation. Most phosphatase enzymes (e.g., alkaline and acid phosphatase and phytase) have a negative fractionation factor, meaning they release phosphate with a depleted δ^{18}O-P (Liang and Blake, 2006b; von Sperber et al., 2014, 2015).

The δ^{18}O-P of available P in the soil can be affected by these processes through various mechanisms. Phosphate ions released by microorganisms to the soil solution potentially contribute a δ^{18}O-P close to isotopic equilibrium, as influenced by the intracellular inorganic pyrophosphatase (Zohar et al., 2010; Poll et al., 2006). Negative offsets from isotopic equilibrium may be caused by the hydrolysis of Po compounds by extracellular or intracellular phosphatase enzymes (Helfenstein et al., 2018). Positive offsets might result from the uptake of phosphate by organisms, as they preferentially take up lighter phosphate isotopologues, thus increasing the δ^{18}O-P of the extracellular phosphate pool (Blake et al., 2005; Lis et al., 2019).

An approach used to detect the main biological processes affecting soil P cycling consists of labeling the soil solution with ^{18}O-enriched water (Bauke et al., 2017; Siebers et al., 2018; Siegenthaler et al., 2020). Enzyme-mediated processes inducing the P–O bond cleavage are therefore detected by tracing the incorporation of O from water into specific phosphate pools.

Tracing P fluxes with this approach is possible provided that the process generating the P flux does not induce a cleavage of the P–O bond, i.e., phosphate is transferred as intact molecule. Abiotic processes, such as sorption/desorption and precipitation/dissolution meet this condition. Additionally, phosphate ions are sorbed or precipitate with negligible isotopologues discrimination (Liang and Blake, 2006b; Jaisi et al., 2010). Through these abiotic processes, the δ^{18}O-P of phosphate acquired via biological processes can be transferred to other inorganic P pools present in the solid phase. This was observed in a study on Andosols along a rainfall gradient, where P bound to calcium was found to carry an equilibrium isotopic signature after losing the δ^{18}O-P of the original parent material (Helfenstein et al., 2018).

Within the German Priority Program SPP1685 "Ecosystem Nutrition: Forest Strategies for Limited Phosphorus Resources" we studied P dynamics and the biological contribution to P availability in organic horizons (Oe) of two contrasting (low- and high-P availability) and well-characterized soils from temperate forests. We chose organic horizons, as they are essential for the recycling of nutrients in forests, supplying up to 99% of plant P demand where inorganic P availability is low (Brandtberg et al., 2004; Jonard et al., 2009; Hauenstein et al., 2018).

We labeled the soil with ^{18}O-enriched water and measured the δ^{18}O-P from different soil P pools in the presence or absence of added leaf litter at several time points during 3 months of incubation. In parallel, we conducted an identical incubation with ^{33}P to quantify P fluxes, as reported in Pistocchi et al. (2018). The results of the present study will be discussed also in relation to this parallel study and the analysis of microbial community composition of Mészáros et al. (2020).

Our hypothesis was that under low P availability, the prevalence of Po mineralization on P fluxes would cause a negative offset in the δ^{18}O-P of the available P due to the negative fractionation of phosphatase enzymes. Under high P availability conditions, we expected the δ^{18}O-P of available P pool to be affected by either (i) abiotic exchanges with mineral phases: in this case, we would observe no incorporation of oxygen from water into phosphate; or (ii) microbial P turnover: in this case, the δ^{18}O-P of the available P would approach isotopic equilibrium. Additionally, we measured the δ^{18}O-P in alkaline and acid-extractable P to trace abiotic exchanges of these pools with the available P. Finally, we made the hypothesis that O incorporation from labeled water into P pools is proportional to microbial activity as suggested by Melby et al. (2013).

MATERIALS AND METHODS

Sites, Soil Sampling and Preparation

The soil organic horizons come from two European Beech forest sites in Germany (*Fagus sylvatica* L., 100–120 years old). The site Bad Brückenau (BBR) is located at about 800 m above sea level (asl) in Northern Bavaria (50°21′7.26″N, 9°55′44.53″E). The site Lüss (LUE) is located at 100 m asl in Lower Saxony (52°50′21.77″N, 10°16′2.37″E). The soils are classified as Dystric Skeletic Cambisol (Hyperhumic, Loamic; IUSS Working Group WRB, 2006) and developed on basalt bedrock, and as a Hyperdystric Folic Cambisol (Arenic, Loamic, Nechic, Protospodic), developed on Pleistocene sand, respectively. The texture of the mineral topsoil in BBR is silty clay loam, while in LUE is loamy sand. A detailed description of the two sites is reported in Lang et al. (2017).

At each site, we collected samples from the leaf litter deposited during the previous autumn and from the organic horizons, in April, 2015 at LUE and May, 2015 at BBR. Litter was collected from the soil surface, and then five to six subsamples were taken from the Oe horizon at each site and bulked into a composite sample (hereafter referred to as BBR and LUE *soil*, respectively).

The soil was sieved while moist to < 5 mm. The litter was dried at 35°C, manually crushed and sieved twice to collect the fraction between 20 and 5 mm. Soil and litter samples were stored at 4°C for a period of 2 weeks (BBR) to 1 month (LUE) before the experiment.

The gravimetric water content of field moist soil was determined by drying for 20 h at 105°C. The water holding capacity (WHC) of the field moist soils was determined by saturating the soils with water and then allowing gravitational water to drain by putting them in a sand bath for 4 h.

Experimental Design and Incubation Experiment

The soils were split in two and two incubations were undertaken. The first was the labeling experiment with ^{18}O enriched water. The second was a soil respiration experiment to measure CO_2 produced as an indicator of microbial activity under the same condition of the labeling experiment. The two incubations lasted 93 and 97 days, respectively.

In both cases, the experiment design had two factors: the soil (BBR and LUE) and the litter treatment, which included the absence [non-amended treatment (NL)] or presence [leaf-litter amended treatment (L)] of leaf litter amendment. All treatments were replicated three times for the labeling experiment and four times for the respiration experiment.

Before splitting the soil, a 3-week pre-incubation at approximately 40% of the maximum WHC was undertaken, during which we monitored the respiration to obtain constant soil respiration rates (Oehl et al., 2001).

For the labeling experiment, soils were weighed in polyethylene zip lock bags (equivalent of 108 g dry soil each) and randomly assigned to the treatments. The labeling solution was prepared with 98% ^{18}O-enriched water (Sercon Limited, Crewe, United Kingdom, the final δ^{18}O in the labeling water was = 34.30‰). Three ml of the labeling solution was added to each of the three replicate bags, spread on the top of the soil by pipetting and then mixed for 1 min by hand through agitating the bag. This process was then repeated to add a total of nine and 12 ml of labeling solution per bag, for BBR and LUE soils, respectively. The added volumes increased the BBR and LUE soils water content to approximately 50% of their WHC. Finally, litter was added to half of the bags, in the ratio of 10 mg per g of dry soil, equivalent to 4.6 mg C g^{-1} soil, which corresponds approximately to natural leaf litter inputs at the two sites (Lang et al., 2017). The bags were left slightly open and arranged in a completely randomized design, in plastic trays which were covered and incubated in the dark at 19°C. To reduce evaporation, which affects the δ^{18}O of soil water, the air moisture was kept approximately constant by placing a beaker with water in each tray.

The labeling experiment was combined with sequential extractions. Concentrations of P were measured in resin-extractable P (inorganic available P, hereafter referred to as P$_{res}$) and hexanol-labile P pools (P$_{hex}$) at days 0, 4, 11, 29, and 93 after labeling. Additionally, at days 0, 4, and 93 we performed a modified Hedley sequential extraction (Tiessen and Moir, 1993; Tamburini et al., 2018) to follow the fate of ^{18}O into other P pools (see section "Soil Phosphorus Pools Concentrations").

For the soil respiration experiment, a set of subsamples (10 g dry weight equivalent) including all soil × litter treatment combinations was prepared on day 0 adding ultrapure H_2O instead of the labeling solution. Each sample was placed in an air-tight jar (1 L volume) with an alkaline trap made of 20 ml 0.2 M NaOH solution, including four blanks without soil. The

jars were then incubated together with the labeled samples. The CO_2 emitted by the soil was measured at weekly intervals by back titration of the trapping solution (Alef, 1995).

Analytical Methods

Soil General Characteristics and Phosphatase Activity

For a detailed description of soil general characteristics and of the corresponding analytical methods refer to Pistocchi et al. (2018).

Potential acid and alkaline phosphatase activities were determined on soil/water suspensions by microplate fluorescence assay (Marx et al., 2001; Poll et al., 2006). A 4-methylumbelliferon (MUF) substrate was added to six replicates of soil/water suspensions under either acidic (pH 6.1) or alkaline (pH 11) conditions. Fluorescence was read on a fluorescence plate reader (Biotek FLx800, Fisher Scientific GmbH, Schwerte, Germany). The analysis was done on 1 g dry weight equivalent samples taken at days 0, 4, 11, 29, and 93 and subsequently frozen until analyzed.

Soil Phosphorus Pools Concentrations

The Hedley sequential extraction scheme was upscaled and adapted for δ^{18}O-P analysis (Tamburini et al., 2018). The initial step of the sequential extraction follows the method proposed by Kouno et al. (1995) and modified by Bünemann et al. (2004). First, two moist soil subsamples were treated in parallel: one subsample was extracted with anion exchange resins (BDH #55164, 12 cm × 4 cm, P_{res}), the other was fumigated with liquid hexanol and extracted with anion exchange resins (P_{hex}). In the upscaled version, the amount of soil, resins and hexanol were adapted to obtain sufficient amount of P for isotope analyses, e.g., up to 100 g equivalent dry soil for LUE, keeping the solid to liquid ratio 1:15 (Tamburini et al., 2018). We did not include a P spiked subsample for quantifying the P recovery according to the method, as this was done in the parallel experiment with ^{33}P tracing (Pistocchi et al., 2018). The P_{res} is a proxy of the available P, while the difference between P_{hex} and P_{res} provides an estimate of the microbial P (P_{mic}).

The soil residue of the subsample extracted with hexanol was used for the subsequent steps of the sequential extraction. First, it was extracted with NaOH/EDTA, targeting the inorganic and organic P bound to Fe and Al oxides (hereafter Pi_{NaOH} and Po_{NaOH}). After removing the resins, NaOH and EDTA disodium salt were added to the soil suspensions in solid form to reach the required concentration (0.25 M NaOH and 0.05 M EDTA). After 16 h shaking, the samples were centrifuged (5300 g for 15 min), filtered through Millipore nylon filters (0.8 μm), and the filtrates were collected for Pi_{NaOH} and Po_{NaOH} determination and purification for isotopes analyses.

Subsequently, the soil residue was extracted with 1 M HCl, targeting sparingly soluble P bound to Ca (Pi_{HCl}), but in acidic soil likely including P bound to Fe and Al oxyhydroxides not entirely extracted during the previous step (Werner et al., 2017). A volume of 1 M HCl was added to the soil residue in the proportion of 10–1 and the extracts collected after shaking overnight and filtering using glass fiber filters (0.8 μm, Millipore).

The concentrations of P_{res}, P_{hex}, Pi_{NaOH}, and Pi_{HCl} were determined colorimetrically (UV-1800, Shimadzu, Canby,

United States) with the malachite green method (Ohno and Zibilske, 1991). The organic fraction, Po_{NaOH}, was determined by difference with the total P concentration in the NaOH–EDTA extract, measured after liquid digestion with concentrated nitric acid and potassium persulfate.

Oxygen Isotopic Values

Oxygen isotopic values in soil water and phosphate

Soil water was quantitatively extracted by cryogenic vacuum extraction (Orlowski et al., 2013) for each combination of soil per treatment at days 0, 4, 11, 29, and 93 after labeling. Oxygen isotopic composition of the soil water (δ^{18}Ow) was measured by equilibration with CO_2 using a gas bench (Thermo Scientific GasBench II) connected to an isotope ratio mass spectrometer (Thermo Scientific Delta V plus) at the facilities of the Department of Earth Science of the ETH Zürich (Seth et al., 2006). Calibration was made with international standards SMOW (Standard Mean Ocean Water), SLAP (Standard Light Antarctic Precipitation), and GISP (Greenland Ice Sheet Precipitation), distributed by the International Atomic Energy Agency (IAEA, Vienna, Austria). Results are reported in the standard delta notation (δ^{18}O) as per mill deviation to the Vienna Standard Mean Ocean Water (VSMOW). Reproducibility of the measurements based on repeated measurements of internal standards was better than 0.03‰.

The P_{res}, P_{hex}, and Pi_{HCl} extracts were purified following the protocol of Tamburini et al. (2010) and modified by Pistocchi et al. (2014). In NaOH–EDTA extracts, both Po_{NaOH} and Pi_{NaOH} are present and a separation prior the purification is needed. According to Tamburini et al. (2018), the NaOH–EDTA pool was divided into high-molecular weight (mostly organic) and low-molecular weight (mostly inorganic) compounds using size exclusion gel chromatography with a Sephadex G25 Medium, presenting a 5 KDa cut-off (ÄKTAprime plus, GE Healthcare Bio-Sciences AB, Uppsala, Sweden). The inorganic pool was purified following the standard protocol, after a precipitation of magnesium ammonium phosphate, which targets inorganic P. The organic pool was hydrolysed by UV radiation, with one split containing ^{18}O-enriched water to check for possible incorporation of O into the newly formed inorganic phosphate.

The P concentration in NaOH–EDTA extracts from LUE was not high enough for the separation–purification procedure and therefore only the δ^{18}O-P values of the initial Po_{NaOH} (δ^{18}O-Po_{NaOH}) are presented.

Purified phosphate in the form of Ag_3PO_4 was weighted in silver capsules in two or three analytical replicates each consisting in 300–600 μg of Ag_3PO_4 and a small amount of glassy carbon powder. Samples were analyzed on a thermal conversion elemental analyzer (vario PYRO cube, Elementar Analysensysteme GmbH, Langenselbold, Germany), coupled to an IsoPrime 100 isotopic ratio mass spectrometer (IRMS) at the Laboratory of the Plant Nutrition Group (ETH Zürich). In each run, repeated measurements of internal Ag_3PO_4 standard (Acros Organics, Geel, Belgium, δ^{18}O = 14.2‰), two benzoic acid international standards (IAEA 601: δ^{18}O = 23.1‰, IAEA 602 δ^{18}O = 71.3‰), and in-house made standards were included for instrumental drift correction

and calibration. The δ^{18}O composition is expressed in the delta notation with respect to VSMOW (Vienna Standard Mean Ocean Water). The δ^{18}O-P of a specific P pool is referred to as: δ^{18}O-P$_{pool\ identification}$. Analytical uncertainties, as determined from the replicate analysis of the standards, were of 0.4‰.

Oxygen isotopic values in leaf litter
Samples of the LUE and BBR leaf litter used in the incubation were extracted and purified according to the protocol of Tamburini et al. (2018). The protocol targets two pools extracted sequentially: the metabolic Pi with trichloroacetic acid (TCA) and the organic P with NaOH–EDTA. In detail, plant material weighed in duplicate (6 g each) was first crushed with the help of liquid N_2 and then extracted with either ^{18}O-labeled or unlabeled 0.3 M TCA. The supernatants were separated after homogenization with a Polytron (Kinematica AG, Lucerne, Switzerland) and shaking (0.5 h) via filtration with glass fiber filters (APFF04700 Merck Millipore). The residue was further extracted with 0.25 M NaOH – 0.05 M Na$_2$(EDTA)$_2 \cdot$H$_2$O, following the protocol described in Noack et al. (2014).

The TCA and NaOH–EDTA supernatants were measured for Pi (Pi$_{TCA}$, Pi$_{NaOH\_litter}$) and Po (Po$_{TCA}$, Po$_{NaOH\_litter}$) and purified for δ^{18}O-P analysis, following the procedure described by Pfahler et al. (2013) and Tamburini et al. (2018), respectively.

Data Analyses
Expected δ^{18}O-P at Isotopic Equilibrium and From Organic P Hydrolysis
The expected δ^{18}O-P of phosphate in equilibrium with soil water (δ^{18}O-P$_{eq}$) was calculated for each time point rearranging the equation from Chang and Blake (2015) as follows:

$$\delta^{18}O\text{-}P_{eq} = e^{\wedge}(14.43/T + 26.54/1000)$$
$$* (\delta^{18}Ow + 1000) - 1000 \qquad (1)$$

where T is the temperature in K during the incubation and δ^{18}Ow (‰) is the measured oxygen isotopic composition of soil water.

The expected δ^{18}O-P of phosphate released from hydrolysis of phosphoesters (δ^{18}O-P$_{Pase}$) via phosphatase enzymes was calculated according to this equation:

$$\delta^{18}O\text{-}P_{Pase} = x \times (\delta^{18}O\text{-}Po) +$$
$$(1 - x) \times (\delta^{18}Ow + \varepsilon) \qquad (2)$$

where x is the proportion of O atoms inherited from the phosphate group in the Po compound (0.75 for phosphomonoester and 0.5 for phosphodiester), δ^{18}O-Po (‰) is the O isotopic composition of the phosphate group in the Po compound, δ^{18}Ow (‰) is the measured O isotopic composition of soil water, and ε (‰) is the enzyme-specific fractionation factor. Here we estimated δ^{18}O-Po as the measured isotopic composition of Po extracted by NaOH–EDTA (δ^{18}O-Po$_{NaOH}$) either from soil or leaf litter (see **Table 1** and sections "Oxygen isotopic values in soil water and phosphate" and "Oxygen isotopic values in leaf litter").

Calculation of δ^{18}O-P
The oxygen isotopic composition of phosphate in the P$_{mic}$ pool (δ^{18}O-P$_{mic}$), was calculated with a mass balance equation (Tamburini et al., 2012):

$$\delta^{18}O\text{-}P_{mic} = (\delta^{18}O\text{-}P_{hex} \times P_{hex} - \delta^{18}O\text{-}P_{res} \times P_{res})/$$
$$(P_{hex} - P_{res}) \qquad (3)$$

where δ^{18}O-P$_{hex}$ (‰) and δ^{18}O-P$_{res}$ (‰) are the oxygen isotopic composition of phosphate in the hexanol and resin extracts, respectively, and P$_{hex}$ (mg P kg^{-1}) and P$_{res}$ (mg P kg^{-1}) are the P concentrations in the corresponding extracts. When δ_{18}O-P$_{hex}$ and δ_{18}O-P$_{res}$ were close, i.e., a difference of less than twice the standard deviation of analytical replicates (< 0.8‰), the δ^{18}O-P$_{hex}$ was taken directly as δ^{18}O-P$_{mic}$. We did not apply any conversion factor (Kp) to correct for incomplete recovery of P$_{mic}$ due to possible ineffectiveness of the fumigant. Indeed, we cannot assume that all P$_{mic}$ compartments, including the ones non-extractable with hexanol, have the same isotopic composition.

Some extractions were done in duplicate with ^{18}O labeled and unlabeled reagents, i.e., TCA, UV digestion of the organic pool of NaOH–EDTA and HCl, to track the incorporation of labeled oxygen into the δ^{18}O-P via inorganic hydrolysis (Tamburini et al., 2010). If incorporation was detected, the actual δ^{18}O-P was calculated according to Pistocchi et al. (2017):

$$\delta^{18}O\text{-}P = (\delta^{18}O\text{-}P_l \times \delta^{18}Ow_{nl} - \delta^{18}O\text{-}P_{nl} \times \delta^{18}Ow_l)/$$
$$(\delta^{18}O\text{-}P_l - \delta^{18}O\text{-}P_{nl} - \delta^{18}Ow_l + \delta^{18}Ow_{nl}) \qquad (4)$$

where δ^{18}O-P$_l$ (‰) and δ^{18}O-P$_{nl}$ (‰) are the oxygen isotopic composition of phosphate for the labeled and unlabeled samples, respectively, and accordingly δ^{18}Ow$_l$ (‰) and δ^{18}Ow$_{nl}$ (‰) the oxygen isotopic composition of labeled and unlabeled extraction solution. When hydrolysis was negligible, as in most cases, the subsamples were considered as duplicates.

Incorporation of O From Water Into Phosphate
Through the process of labeling with ^{18}O-enriched water, it is possible to calculate how much O from soil water was incorporated into phosphate molecules of a specific P pool over time. Oxygen incorporation (%) was calculated as the slope of the straight line between two points in the δ^{18}Ow-δ^{18}O-P plot (Liang and Blake, 2006a):

$$O\ incorporation = (\delta^{18}O\text{-}P_t - \delta^{18}O\text{-}P_{t0})/$$
$$(\delta^{18}Ow_t - \delta^{18}Ow_{t0}) \times 100 \qquad (5)$$

Where δ^{18}Ow$_t$ and δ^{18}Ow$_{t0}$ are the oxygen isotopic compositions of soil water and δ^{18}O-P$_t$ and δ^{18}O-P$_{t0}$ are the oxygen isotopic compositions of phosphate in a given pool at time point t and at day 0, respectively.

Incorporations of 25 or 50% indicate that overall one out of four or two out of four O atoms, respectively, are incorporated from water into phosphate. 100% O incorporation indicates all four O of phosphate derived from water.

For δ^{18}O-P values obtained with the Equations 3, 4, and 5 the mean and standard deviation per sample were obtained with a Monte Carlo error propagation simulation (Anderson, 1976).

TABLE 1 | General characteristics of the two studied Oe horizons at site Lüss (LUE) and Bad Brückenau (BBR).

Soil Property or Variable	Unit	LUE	BBR
Humus form and humus layer thickness	–	Mor-like Moder (13 cm)	Mull-like Moder (5 cm)
Water holding capacity	g g^{-1}	2.92	3.26
pH$_{H2O}$	–	3.55	3.70
Organic Carbon	g C kg^{-1}	364	237
Organic Nitrogen	g N kg^{-1}	16.7	14.8
Microbial Carbon (C$_{mic}$)	mg C kg^{-1}	1,047	844
Microbial Nitrogen	mg N kg^{-1}	238	152
Microbial P (P$_{mic}$)	mg P kg^{-1}	55.6	98.8
Total P	mg P kg^{-1}	485	2,564
Organic P	mg P kg^{-1}	371	1,523
Available P (P$_{res}$)	mg P kg^{-1}	3.0	34.7
Corg: Norg	mol/mol	25.4	18.7
C$_{mic}$: N$_{mic}$	mol/mol	5.1	6.5
Corg: Porg	mol/mol	2,949	426.4
C$_{mic}$: P$_{mic}$	mol/mol	48.6	21.1
Acid phosphatase potential activity (day 1)	nmol g^{-1} h^{-1}	19,207	16,098
Alkaline phosphatase potential activity (day 1)	nmol g^{-1} h^{-1}	146	74
Metabolic quotient (cCO$_2$; 1)	μg C–CO$_2$ μg^{-1} Cmic h^{-1}	4.5	2.6
δ_{18}O-P of organic P (2)	‰	22.47	17.22
δ_{18}O-P of leaf litter, TCA (3)	‰	13.48	17.06
δ_{18}O-P of leaf litter, NaOH (3)	‰	20.42	18.58

(1) Unit CO$_2$ respired per unit microbial carbon. Calculated using steady respiration rate measured in the present study. (2) Oxygen isotopes composition of organic P from 25 M sodium hydroxide – 0.05 M sodium EDTA soil extract. (3) Oxygen isotopes composition of P in leaf litter, TCA, 0.3 M Trichloroacetic acid extract; NaOH, 0.25 M sodium hydroxide – 0.05 M sodium EDTA extract.

Calculations were repeated 10 million times by varying the δ_{18}O signatures according to their mean and standard deviations. For the δ_{18}Ow$_s$, we assumed a standard deviation of 0.03‰ corresponding to the analytical error.

Statistical Analyses

A two-way ANOVA (1st factor = litter application, 2nd factor = date) was applied to analyze the variables measured during the incubation for each soil separately except the respiration rates. These latter were analyzed with a mixed model, where the litter amendment was the fixed factor and the time of the measurement (weekly) a random factor with the replicate nested in it. Model simplification (one-way ANOVA) was done when possible or when data were missing, e.g., δ_{18}O-Po$_{NaOH}$ in LUE soil. In some cases, there were not enough replicates for statistical tests. These results are discussed qualitatively. The Tukey test was used for *post hoc* comparison. The Student's paired *t*-test was used when comparing single dates and cumulative values, after checking for homogeneity of variances. The Shapiro–Wilk test was used to assess normality of the data. All analyses were performed in R 3.1.1 (R version 3.1.1, R Core Team).

RESULTS

Soil Respiration

The soil respiration declined during the first 3–4 weeks by approximately 10 and 25% for LUE and BBR soils, respectively. After the first month, the respiration remained approximately constant (**Figure 1**). The soil respiration of LUE soil was almost double that of the one measured for BBR soil. Similarly, the

metabolic quotient cCO$_2$, calculated with the average respiration rates over the last 8 weeks, was almost double in LUE soil (**Table 1**).

During the first 4 weeks, differences between treatments were detectable, with leaf litter-amended soils showing higher respiration rates (**Figure 1**). This resulted in a cumulative additional carbon (C) release for the litter-amended soils of 3.4 and 11.1% for LUE and BBR soils, respectively, significant only for the latter (**Supplementary Table 1 SI**).

Soil General Characteristics and Potential Phosphatases Activity

The two soils were acidic (3.77 and 3.65 for BBR and LUE soil, respectively) but differed in almost all considered variables (**Table 1**). In particular, concentration of total, organic and available P was much higher in BBR than in LUE soil.

Potential acid phosphatase activity was similar for LUE and BBR soils, while potential alkaline phosphatase activity was double in LUE soil, although much lower than the acid phosphatase activity (**Table 1** and **Supplementary Figure 1SI**). Therefore, for the calculation of the expected value from Po hydrolysis by phosphatases with Equation 2 we used the fractionation factor (ε) of – 10‰ attributed to acid phosphatases (von Sperber et al., 2014). No differences were found between litter treatments.

The Concentration and δ_{18}O-P of Resin-Extractable and Microbial P Pools

In both LUE and BBR soils the concentration of P$_{res}$ increased, while P$_{mic}$ remained largely stable over the study time with small

FIGURE 1 | CO_2 emitted from Lüss (LUE; **A**) and Bad Brückenau (BBR; **B**) soils during the incubation. Gray circles indicate respiration rates during the pre-incubation period, white circles the respiration rates in the non-amended treatment (NL) and black circles in the leaf-litter amended treatment (L). Error bars indicate replicates standard deviation.

FIGURE 2 | The δ^{18}O-P of available P (P_{res}) and microbial P (P_{mic}) pools in Lüss (LUE; **A**) and Bad Brückenau (BBR; **B**) soils over the course of the incubation. The expected isotopic equilibrium between phosphate and water (Equation 1) is indicated by the red dotted line and the expected isotopic signature of phosphate from organic P (Po) hydrolysis of soil organic matter via acid phosphatase (Equation 2) is indicated by the green dotted line. Error bars indicate replicates standard deviation. NL, non-amended; L, leaf litter-amended.

fluctuation in the low P LUE soil and decreased significantly in the high P BBR soil (**Supplementary Table 2 SI**). In the litter-amended BBR soil the P_{res} was slightly higher, with a mean effect size of $+ 2.1$ mg kg^{-1}. The litter addition increased the P_{mic} slightly in both soils, with a mean effect size of $+ 4.9$ and $+ 4.4$ mg kg^{-1} for LUE and BBR, respectively (**Supplementary Table 2 SI**).

The δ^{18}O-P_{res} and δ^{18}O-P_{mic} increased by several units during the incubation in both LUE and BBR soils (**Figure 2**). Therefore, incorporation of O from labeled soil water into phosphate occurred.

For the low P LUE soil, both δ^{18}O-P_{res} and δ^{18}O-P_{mic} had a similar initial value (13.9 and 12.7‰, respectively) and

both followed a slight increasing trend over the duration irrespective of the application of leaf litter. This change in value was similar to that predicted by the δ^{18}O-P_{Pase}, i.e., expected from the hydrolysis of Po via acid phosphatases (Equation 2; **Figure 2A**).

For the high P BBR soil, however, the initial values of δ^{18}O-P_{res} and δ^{18}O-P_{mic} were different: 19.9‰ vs. 14.0‰, respectively. The δ^{18}O-P_{mic} increased slightly over time and remained below the expected equilibrium between phosphate and water (δ^{18}O-P_{eq} in Equation 1), whereas the δ^{18}O-P_{res} approached and exceeded the δ^{18}O-P_{eq} by day 93 (**Figure 2B**). The δ^{18}O-P_{mic} values were in average lower for the non-amended treatment ($p < 0.05$).

For both soils, the picture does not change if we consider the δ^{18}O-P_{Pase} values calculated using the Po in the litter, as they are similar to the ones from soil Po (see δ^{18}O-P_{Pase} litter, **Supplementary Table 2 SI**).

The Concentration and δ^{18}O-P of NaOH- and HCl-Extractable Pools

In the LUE soil incubation, concentrations of the inorganic pools Pi_{NaOH} and Pi_{HCl} remained approximately stable during the incubation. The organic pool, Po_{NaOH}, increased slightly ($+ 36.8$ mg kg^{-1} at day 93). No differences were detected between the litter amended and non-amended treatments (**Table 3**).

In BBR, a slight increase (mean effect size of $+ 49.0$ mg kg^{-1} at day 93) of the Pi_{NaOH} was registered over the incubation time. The Pi_{HCl} and Po_{NaOH} remained stable over the incubation time. No differences due to the leaf litter addition were observed (**Table 3**).

The δ^{18}O-Pi_{HCl} in the LUE soil incubation had a slight increase ($+ 1\permil$). We could not analyze the δ^{18}O-Pi_{NaOH} or δ^{18}O-Po_{NaOH} in LUE soil because of the insufficient amount of P extracted. In the BBR soil, we detected a significant increase of the δ^{18}O-P of both inorganic and organic pools. The δ^{18}O-Pi_{NaOH} increased by $4.4\permil$, as an average of the L and NL treatments. A similar increase was measured for the δ^{18}O-Pi_{HCl} (**Table 3**). Despite those increases neither δ^{18}O-Pi_{NaOH} nor δ^{18}O-Pi_{HCl} reached the corresponding value of the available P (P_{res}) at day 93, meaning that they did not completely equilibrate with the P_{res} at the end of the incubation. Similarly, the δ^{18}O-Po_{NaOH} also increased slightly, but by only approximately $1\permil$ at the end of the incubation.

Differences due to the litter addition were found in the BBR soil for the δ^{18}O-Po_{NaOH} ($+ 1\permil$ for the L treatment at day 4) and for the δ^{18}O-Pi_{HCl} ($-2.3\permil$ for the L treatment at day 93).

^{18}O Incorporation Into P Pools

The addition of ^{18}O-enriched water successfully increased O isotopic ratio of soil water (**Supplementary Table 3 SI**) and resulted in incorpora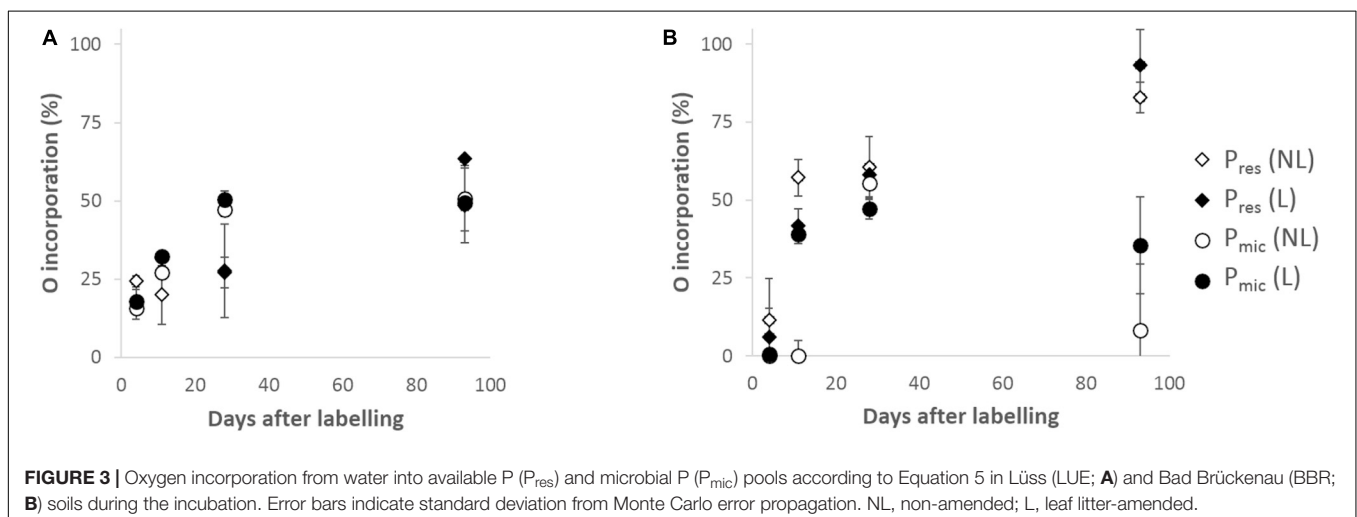tion of ^{18}O from water into major soil P pools. The trend, however, differed in the two soils. In LUE, both the P_{res} and P_{mic} incorporated O at similar rate: around one out of four O atoms per phosphate (25%) were exchanged in the first 20–30 days of incubation and up to two out of four (50%) were exchanged after 93 days (**Figure 3A**). In BBR instead, the ^{18}O from water was incorporated faster, but it did not exceed 50% in the P_{mic} by day 93, while it had reached 90% in the P_{res}, suggesting an almost complete exchange of the four O of phosphate with water (**Figure 3B**). A decline of the O incorporation in P_{mic} in the BBR soil was observed between the second-last and the last sampling. This decline was more pronounced in the treatment without litter. A stronger relationship was found between O incorporation in Pres and cumulated respiration in BBR soil as compared to LUE (**Figure 4A**).
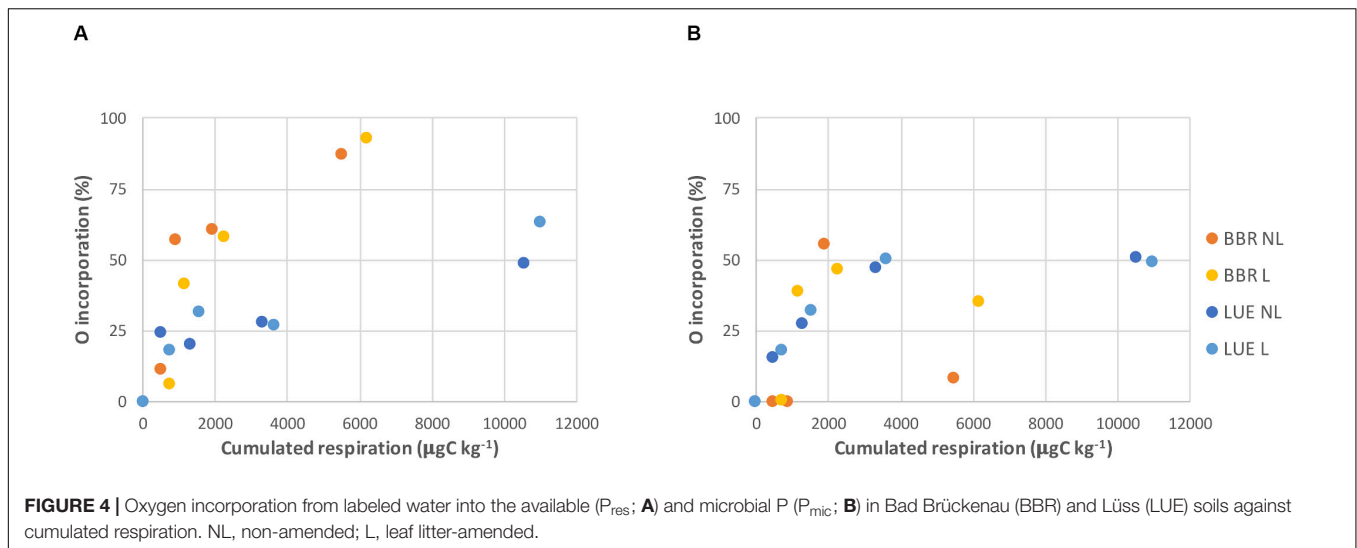
DISCUSSION

The increase in δ^{18}O-P value of almost all P pools indicates that biological processes were involved in P cycling in both soils, as the exchange of oxygen between soil phosphate and water involves enzymatic reactions (Tudge, 1960).

Biological Processes Affecting Available P in the Low P Availability LUE Soil

Under low P availability, δ^{18}O-P_{mic} and δ^{18}O-P_{res} were very similar and followed the same temporal trend (**Figure 2A**). There are three potential explanations for this pattern: (i) There was phosphate efflux from P_{mic} to P_{res}, so the P_{res} pool was strongly influenced by the P_{mic} pool as observed in other P-poor soils (Tamburini et al., 2012; Weiner et al., 2018); (ii) There was no phosphate efflux from P_{mic} to P_{res}, but the dominant enzymatic processes were the same in both pools, thus imprinting the same isotopic signature; finally (iii) There was no phosphate efflux from P_{mic} to P_{res}, and the two pools were impacted by different enzymatic processes which resulted in similar δ^{18}O-P just by chance.

FIGURE 3 | Oxygen incorporation from water into available P (P_{res}) and microbial P (P_{mic}) pools according to Equation 5 in Lüss (LUE; **A**) and Bad Brückenau (BBR; **B**) soils during the incubation. Error bars indicate standard deviation from Monte Carlo error propagation. NL, non-amended; L, leaf litter-amended.

FIGURE 4 | Oxygen incorporation from labeled water into the available (P$_{res}$; **A**) and microbial P (P$_{mic}$; **B**) in Bad Brückenau (BBR) and Lüss (LUE) soils against cumulated respiration. NL, non-amended; L, leaf litter-amended.

The parallel ^{33}P dilution experiment showed that gross mineralization strongly contributed to the P$_{res}$ pool. It also highlighted a fast and important P immobilization into the microbial biomass (around 95% of gross mineralization, see Pistocchi et al., 2018). The ^{33}P experiment, however, gave no direct evidence of an efflux from P$_{mic}$ to P$_{res}$. This may point either to the first or to the second explanation. Lis et al. (2019) observed in an *in vitro* experiment that cyanobacteria growing under P-depleted conditions took up P through phosphate specific transporters (Pst) without leaking it. Therefore, the second explanation, i.e., no or little phosphate efflux from P$_{mic}$ to P$_{res}$ and same dominant enzymatic processes, is more likely (see **Figure 5A** modified after Lis et al., 2019). However, compared to their study we did not observe isotopic equilibrium in the intracellular and extracellular P.

Of further consideration is that both δ^{18}O-P$_{mic}$ and δ^{18}O-P$_{res}$ were similar to the value expected for phosphomonoester hydrolysis over the first 30 days of incubation (one out of four O was exchanged with water, see **Figure 2A**). According to a two end-members mass balance including the isotopic equilibrium (δ^{18}O-P$_{eq}$, Equation 1) and the δ^{18}O-P$_{Pase}$ (Equation 2), this contribution represented almost 100% of the P$_{res}$ over this period.

By the end of the incubation, the O incorporation into P$_{res}$ had attained 50% (two out of four O atoms exchanged with water; **Figure 3A**), suggesting the contribution of other processes. There are two possible explanations: (i) that a single enzymatic process which incorporates two O atoms from water into phosphate was prevailing; or (ii) two or more processes contributed, resulting in 50% average O incorporation. The first explanation would be that the extracellular hydrolysis of phosphodiesters was occurring. However, Lang et al. (2017) found that the potential activity of phosphodiesterases over phosphomonoesterases was very low at this site. The contribution of multiple processes is, therefore, more likely. A two end-members balance including δ^{18}O-P$_{eq}$ and δ^{18}O-P$_{Pase}$ as previously hypothesized, suggests that phosphate derived

from monoester hydrolysis constitutes about 80% of the P$_{res}$ at the end of the incubation. Interestingly, this value agrees with the results of parallel ^{33}P incubation, where 94% of P exchanged with the soil solution came from gross mineralization (Pistocchi et al., 2018).

We conclude that under low P availability, both the P$_{res}$ and the P$_{mic}$ pools were dominated by phosphomonoesterase catalyzed reactions.
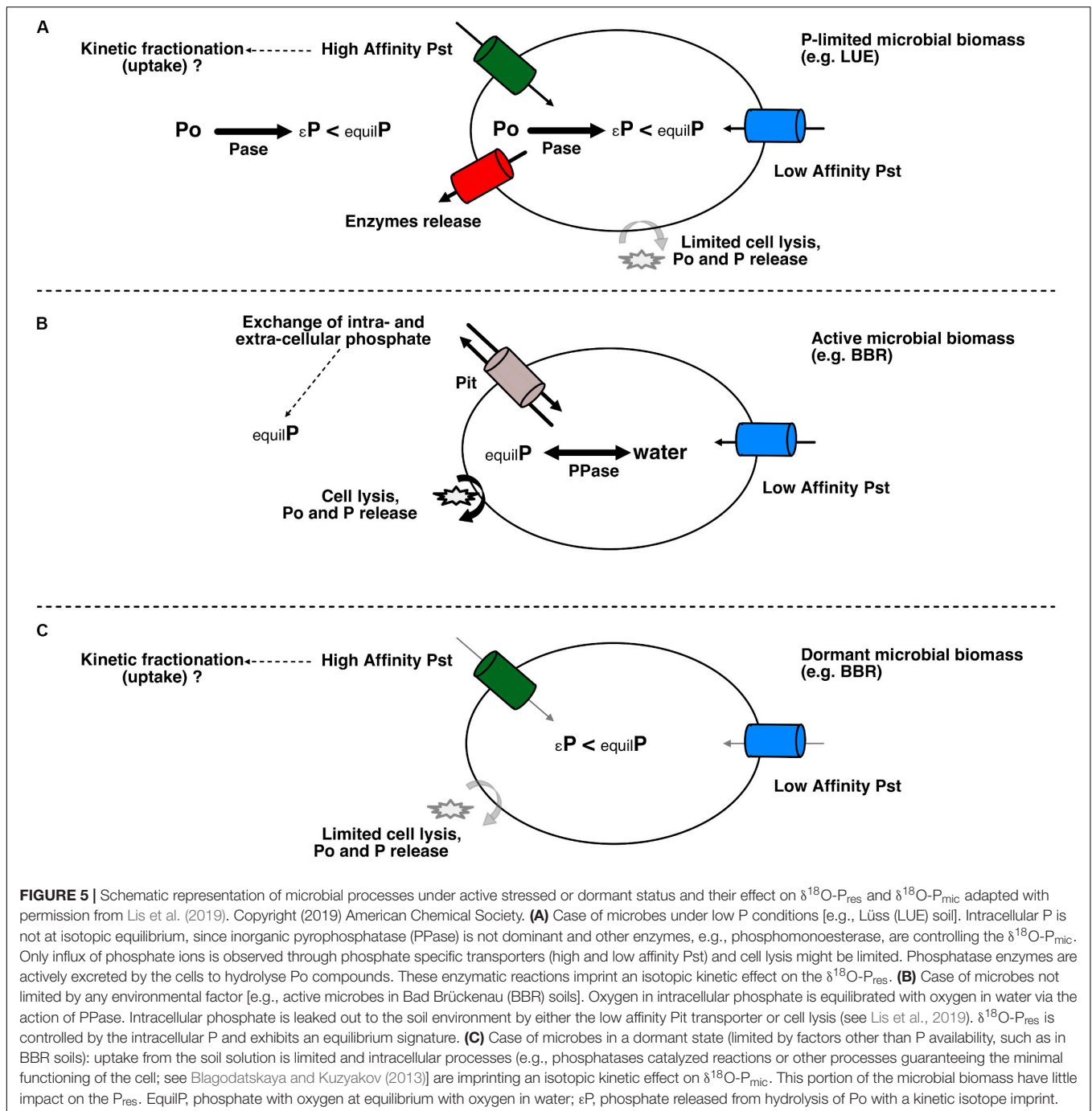
The attainment of the isotopic equilibrium was until now considered the main biological effect influencing the available P, corresponding to P$_{res}$ as defined in this study, via the release of intracellular phosphate ions (Zohar et al., 2010; Tamburini et al., 2012; Stout et al., 2014; Weiner et al., 2018; Lis et al., 2019). Our results support the hypothesis that under P-limiting conditions, the isotopic effect of Po hydrolysis can outweigh the isotopic equilibrium effect driven by inorganic pyrophosphatase in both P$_{mic}$ and P$_{res}$ pools (**Figure 5A**).

Biological Processes Affecting Available P in the High P Availability BBR Soil

Under high P availability, the P$_{res}$ pool carried a very distinct isotopic signature from the P$_{mic}$ pool (**Figure 2B**). The δ^{18}O-P$_{res}$ was close to or higher than the δ^{18}O-P$_{eq}$ (isotopic equilibrium between phosphate and water, Equation 1), while δ^{18}O-P$_{mic}$ was in between δ^{18}O-P$_{eq}$ and the δ^{18}O-P$_{Pase}$ (Equation 2).

The contribution of P from leaf litter does not explain the δ^{18}O-P$_{res}$ values, as we did not find significant differences between litter treatments. The exchange with other soil P pools via sorption/desorption or precipitation/dissolution does not explain them either, as the Pi$_{NaOH}$ and Pi$_{HCl}$ all had lower δ^{18}O-P than δ^{18}O-P$_{res}$ (see **Table 2**), although these P pools likely exchanged phosphate ions with the P$_{res}$ pool (see section "Exchanges Between Available P and Other Inorganic and Organic P Pools").

The incorporation of O atoms from labeled water was around 90% in the P$_{res}$ pool by day 93, suggesting the prevalence of a process that leads to an exchange of all four O atoms. The

FIGURE 5 | Schematic representation of microbial processes under active stressed or dormant status and their effect on δ^{18}O-P$_{res}$ and δ^{18}O-P$_{mic}$ adapted with permission from Lis et al. (2019). Copyright (2019) American Chemical Society. **(A)** Case of microbes under low P conditions [e.g., Lüss (LUE) soil]. Intracellular P is not at isotopic equilibrium, since inorganic pyrophosphatase (PPase) is not dominant and other enzymes, e.g., phosphomonoesterase, are controlling the δ^{18}O-P$_{mic}$. Only influx of phosphate ions is observed through phosphate specific transporters (high and low affinity Pst) and cell lysis might be limited. Phosphatase enzymes are actively excreted by the cells to hydrolyse Po compounds. These enzymatic reactions imprint an isotopic kinetic effect on the δ^{18}O-P$_{res}$. **(B)** Case of microbes not limited by any environmental factor [e.g., active microbes in Bad Brückenau (BBR) soils]. Oxygen in intracellular phosphate is equilibrated with oxygen in water via the action of PPase. Intracellular phosphate is leaked out to the soil environment by either the low affinity Pit transporter or cell lysis (see Lis et al., 2019). δ^{18}O-P$_{res}$ is controlled by the intracellular P and exhibits an equilibrium signature. **(C)** Case of microbes in a dormant state (limited by factors other than P availability, such as in BBR soils): uptake from the soil solution is limited and intracellular processes (e.g., phosphatases catalyzed reactions or other processes guaranteeing the minimal functioning of the cell; see Blagodatskaya and Kuzyakov (2013)] are imprinting an isotopic kinetic effect on δ^{18}O-P$_{mic}$. This portion of the microbial biomass have little impact on the P$_{res}$. EquilP, phosphate with oxygen at equilibrium with oxygen in water; εP, phosphate released from hydrolysis of Po with a kinetic isotope imprint.

only known enzyme which could cause a complete exchange of O atoms with water is the inorganic pyrophosphatase (Cohn, 1958), which is mostly intracellular (Poll et al., 2006). However, the P$_{mic}$ pool in the BBR soil, showed consistently lower O incorporation when compared to the P$_{res}$. The presence of different microorganisms in either active or dormant states, all extracted with hexanol but carrying different isotopic signatures, could possibly explain the difference in δ^{18}O-P between P$_{res}$ and P$_{mic}$ pools. However, only the active microbial community would carry a signature close to δ^{18}O-P$_{eq}$ and contribute to the

P$_{res}$ via P uptake, intracellular turnover and release (Siegenthaler et al., 2020). Indeed, inorganic pyrophosphatase is involved in DNA synthesis, amongst other processes, and therefore is more active when cells are growing (Kottur and Nair, 2018). The microorganisms in a dormant state would interact poorly with the P$_{res}$ pool and incorporate less O from water (see section "δ^{18}O-P and Microbial Activity" for more discussion).

The O incorporation of close to 90% (**Figure 2B**) implies that almost all the phosphate in the final P$_{res}$ pool (i.e., 45.8 and 49.8 mg kg^{-1}, for the NL and L treatment, respectively)

TABLE 2 | Concentration and δ^{18}O-P values of inorganic and organic P pools over the incubation period.

Treatment	Days	δ^{18}O-Pi$_{NaOH}$			δ^{18}O-Po$_{NaOH}$			δ^{18}O-Pi$_{HCl}$			Pi$_{NaOH}$			Po$_{NaOH}$			Pi$_{HCl}$		
		Mean	SD	n	Mean	SD	n	Mean	SD	n	Mean	SD	n	Mean	SD	n	Mean	SD	n
							LUE									LUE			
	0	nm	nm	–	22.47	nm	1	21.82	0.12	2	95	3	3	168	37	3	7.2	0.1	3
NL	4	nm	nm	–	nm	nm	–	19.30	0.29	2	105	3	3	176	17	3	5.7	0.3	3
L	4	nm	nm	–	nm	nm	–	nm	nm	-	106	2	3	150	32	3	5.5	0.3	3
NL	93	nm	nm	–	nm	nm	–	22.68	0.51	2	102	5	3	203	7	3	7.5	1.7	3
L	93	nm	nm	–	nm	nm	–	22.55	0.24	2	105	4	3	206	45	3	5.2	0.3	3
							Time effect									Time effect			
		–			–			***	(1)		ns			*			ns		
							Litter effect									Litter effect			
		–			–			ns	(1)		ns			ns			ns		
							BBR									BBR			
	0	16.52	0.85	2	17.22	0.81	3	17.47	0.36	2	658	9	3	1,320	68	3	98.6	10.2	3
NL	4	18.65	0.80	2	16.90	0.29	3	19.17	nm	1	621	39	3	1,426	118	3	83.4	9.4	3
L	4	18.92	nm	1	17.93	0.91	2	19.23	nm	1	660	10	2	1,386	186	3	81.1	23.7	3
NL	93	21.12	nm	1	18.34	0.38	2	21.94	0.21	3	720	50	3	1,569	342	3	91.1	19.9	3
L	93	22.38	nm	1	18.55	0.37	2	19.67	0.30	3	699	13	3	1,552	248	3	114.7	9.8	3
							Time effect									Time effect			
		***	(1)		**			***			***			ns			ns		
							Litter effect									Litter effect			
		–			*			***			ns			ns			ns		

*Pi$_{NaOH}$, NaOH–EDTA-extractable inorganic P; Po$_{NaOH}$, NaOH–EDTA-extractable organic P; Pi$_{HCl}$, HCl-extractable inorganic P; L, leaf litter-amended; NL, non-amended. Significance levels according to two-way ANOVA, where not differently specified: *** $p < 0.001$; ** $p < 0.01$; * $p < 0.05$; ns, non-significant; nm, not measurable. (1) Significance value from a 1-way ANOVA.*

underwent intracellular P turnover catalyzed by inorganic pyrophosphatases over the investigated period. Part of this efflux from P$_{mic}$ corresponded to a net loss, more pronounced in the NL treatment, which in turn translated in a net increase of P$_{res}$ (**Supplementary Table 2 SI**) and a transfer to other Pi or Po pools (see section "Exchanges Between Available P and Other Inorganic and Organic P Pools").

At the end of the incubation, the δ^{18}O-P$_{res}$ was higher than the expected equilibrium by + 3.0‰. Recent studies on temperate forest soils reported enriched isotopic ratios compared to expected equilibrium after a period of incubation (Gross and Angert, 2017; Weiner et al., 2018). They attributed this positive offset to the steady-state between the efflux of intracellular P at isotopic equilibrium and the P uptake by microbes inducing isotopic enrichment of the extracellular phosphate ions (Blake et al., 2005; Lis et al., 2019). Although this effect could explain our finding, this explanation appears unlikely. Firstly, in our system P$_{res}$ increased during the incubation period, which does not fit into a Rayleigh fractionation model, which describes the kinetic fractionation induced by P uptake (Blake et al., 2005). Secondly, the mentioned studies observed the effect of P uptake by cells mostly under low environmental P conditions, which is not the case in the BBR soil.

It can also not be ruled out that a possible contribution from an unknown extracellular process occurred, leading to the exchange of four O atoms between phosphate and water, and/or the partial contribution of mineralization of Po compounds with heavy δ^{18}O-P.

δ^{18}O-P and Microbial Activity

Saaby Johansen et al. (1991) and Melby et al. (2013) showed a positive relationship between δ^{18}O-P de-labeling and respiration in incubation experiments with addition of ^{18}O-labeled phosphate. Siegenthaler et al. (2020) suggested that a high incorporation of O from labeled water into the P$_{mic}$ pool reflects a high microbial activity.

In this study, we observed a higher respiration rate, therefore a higher microbial activity, in the low P LUE soil when compared to the high P BBR soil. Similarly, the microbial respiration per unit microbial biomass (metabolic quotient, cCO$_2$) of the LUE soil was twice the value recorded for the BBR soil (**Table 1**). In contrast, the O incorporation into the P$_{res}$ per unit CO$_2$ respired was lower in LUE soil (**Figure 4A**).

The dominance of phosphomonoesterase catalyzed reactions in the P$_{res}$ pool of the LUE soil (see section "Biological Processes Affecting Available P in the Low P Availability LUE Soil")

explains the lower O incorporation. This together with the higher cCO_2 might indicate differences in the microbial communities composition and/or a stronger investment of the LUE microbial community into Po mining via the production of extracellular phosphatase enzymes (Manzoni et al., 2010; Spohn and Chodak, 2015). The community composition analyses of Mészáros et al. (2020) and the δ^{18}O-P data of the present study suggest that both factors possibly contribute simultaneously.

The O incorporation into the P_{mic} pool was similar in the two soils during the first month of incubation, then lower in the BBR soil, which showed a strong decrease in the non-amended treatment (**Figures 3B, 4B**).

We assumed earlier (section "Biological Processes Affecting Available P in the High P Availability BBR Soil") that in the BBR soil only part of the microbial community was actively turning over P and imprinting an isotopic equilibrium signature on it. The below-equilibrium δ^{18}O-P_{mic} and corresponding O incorporation resulted, therefore, from the relative contribution of δ^{18}O-P_{mic} at the isotopic equilibrium and δ^{18}O-P_{mic} below isotopic equilibrium. Lower δ^{18}O-P_{mic} would either occur because of the dominance of intracellular phosphomonoesterase reactions or because of little exchange of O between intracellular phosphate and labeled water (Chen et al., 2019). Since the δ^{18}O-P_{mic} was lower than isotopic equilibrium already before the labeling, the first explanation seems more likely. The two typologies outlined in **Figures 5B,C** would, therefore, contribute to the δ^{18}O-P_{mic} in the BBR soil.

The decrease in the O incorporation in the δ^{18}O-P_{mic} of the non-amended BBR soil by the end of the incubation was concomitant with a strong decrease in P_{mic} concentration (**Supplementary Table 2 SI**). These effects could be determined by a decrease in the activity of microbial cells or a shift in the microbial community composition in response to less favorable environmental conditions (Fanin et al., 2013; Mooshammer et al., 2014). The respiration rates were very similar between treatments over the last 2 months of incubation (**Figure 1**). However, the analysis of microbial community composition showed a shift in both the fungal and bacterial communities. Additionally, the bacterial community changed differently in the amended and non-amended treatments over the last incubation

period (Mészáros et al., 2020). The second explanation seems, therefore, more likely.

In LUE the incorporation of O from labeled water into P_{mic} was driven by phosphomonoesterase catalyzed reactions as for P_{res} (see section "Biological Processes Affecting Available P in the Low P Availability LUE Soil"). Pfahler et al. (2013) reported δ^{18}O-P of soybean leaves decreased under P-limiting conditions and suggested this was the result of increased recycling of Po within plant tissue. Therefore, P-limiting conditions might induce a tighter intracellular Po recycling and translate in below-equilibrium δ^{18}O-P_{mic} values (**Figure 5A**). Interestingly, we found below-equilibrium δ^{18}O-P_{mic} also in non-incubated samples taken at the site LUE at two different dates (unpublished results), which suggests this effect is not an artifact of the incubation.

In summary, despite similar below-equilibrium δ^{18}O-P_{mic} in LUE and BBR soils, data such as δ^{18}O-P_{res}, respiration rates and microbial communities composition, suggest a tighter P cycling in LUE. Interestingly, such differences were not reflected in different potential acid phosphatases activities (**Table 1** and **Supplementary Figure 1** in SI). Our data also suggest that the relationship between microbial activity and O incorporation into phosphate is not simply proportional as we initially hypothesized but likely modulated by P availability.

Exchanges Between Available P and Other Inorganic and Organic P Pools

Due to the low extractable P concentration in LUE, we can only discuss results from the BBR soil.

In the parallel ^{33}P experiment the P_{res} and the Pi_{NaOH} were shown to exchange rapidly in the BBR soil, with the tracer found in the Pi_{NaOH} pool after 4 days. This suggests a fast exchange process, such as sorption/desorption. However, 3-months of incubation were not sufficient to attain a complete exchange between these two pools (Pistocchi et al., 2018).

As these exchanges are abiotic, i.e., without P–O bond cleavage, it is possible to trace P fluxes also with the δ^{18}O-P, provided that the two exchanging pools have different initial isotopic signatures.

TABLE 3 | Estimation of P exchange fluxes in the Bad Brückenau (BBR) soil between the available and other inorganic P pools over 93 days according to a mass balance (δ^{18}O-P data from this study) or to an isotopic dilution approach (^{33}P data from Pistocchi et al., 2018).

P pool	Treatment	δ^{18}O-P Mass Balance		^{33}P Isotopic Dilution	
		Proportion of the P pool exchanged (1)	mg kg^{-1} day^{-1} P exchanged	Proportion of the P pool exchanged (2)	mg kg^{-1} day^{-1} P exchanged
Pi_{NaOH}	NL	0.47	3.5	0.47	3.5
	L	0.53	3.9	0.54	4.0
Pi_{HCl}	NL	0.51	0.5	0.29	0.8
	L	0.22	0.3	0.31	0.9

L, leaf litter-amended; NL, non-amended. (1) proportion of the P pool exchanged = $(\delta^{18}O\text{-}P \text{ (target pool)}_{(t)} - \delta^{18}O\text{-}P \text{ (target pool)}_{(0)})/(\delta^{18}O\text{-}P_{res} - \delta^{18}O\text{-}P \text{ (target pool)}_{(0)})$, where 0 and t represent the day 0 and a time t (93 days), respectively, and $\delta^{18}O\text{-}P_{res(t)}$ is the oxygen isotopes ratio of the available P at time t. (2) According to the equation of Fardeau et al. (1995) $q_{(t)} = Q(r_{(t)}/R)$, where $q_{(t)}$ is the proportion of P exchanged in the target pool at time t, r is the radioactivity in the target pool, R is the total radioactivity introduced, and Q is the mass of the labeled pool (in this case the available P).

The increase of the δ^{18}O-Pi$_{NaOH}$ suggests that phosphate ions were transferred from an enriched P pool, presumably P$_{res}$. As was found with the ^{33}P, the Pi$_{NaOH}$ and the P$_{res}$ did not attain similar isotopic compositions by the end of the incubation. On the contrary, their isotopic signature diverged, due to a large increase of the δ^{18}O-P$_{res}$ (see **Table 3** and **Supplementary Table 2 SI**). It would appear that over the time scale of this incubation study, the biological processes that led to the isotopic enrichment of the P$_{res}$ had a stronger effect than the ions exchange with the Pi$_{NaOH}$ pool.

A mass balance, assuming constant P concentrations over the incubation, yields an exchange flux between P$_{res}$ and Pi$_{NaOH}$ of approximately 3.5–3.9 mg kg^{-1} day^{-1}, which is similar to estimates provided by the ^{33}P tracing experiment (**Table 3**).

The δ^{18}O-Pi$_{HCl}$ also increased over time, suggesting an exchange with an isotopically enriched P pool. Similarly, we assume that the Pi$_{HCl}$ exchanged phosphate ions with the P$_{res}$ pool via abiotic reactions, allowing us to trace P fluxes via the δ^{18}O-P. Through a mass balance calculation, we estimated 0.3–0.5 mg kg^{-1} day^{-1} of P was exchanged on average between these two P pools (**Table 3**).

The addition of leaf litter resulted in a slightly lower δ^{18}O-Pi$_{HCl}$ at the end of the incubation (**Table 2**). To explain this, we have to assume that an abiotic transfer of depleted phosphate from the litter to the Pi$_{HCl}$ has occurred. Although the inorganic P in the litter had a slightly depleted δ^{18}O-P (17.06‰ for the TCA extract, see **Table 1**), the amount of inorganic P contained within the litter was small compared to the Pi$_{HCl}$ pool. Furthermore, no other differences in other inorganic P pools of the leaf litter-amended soils were observed. Therefore, we cannot exclude the lower δ^{18}O-P$_{HCl}$ was not simply a processing error.

In summary, the P$_{res}$ exchanged mostly with the Pi$_{NaOH}$ pool, which is in agreement with previous studies on BBR (Lang et al., 2017; Pistocchi et al., 2018) or on low-pH and Fe/Al oxides-rich soils (Buehler et al., 2002; Helfenstein et al., 2020).

The δ^{18}O-Po$_{NaOH}$ increased slightly in the BBR soil (+ 1.1–1.3‰ in the NL and L treatment, respectively). The effect of leaf litter on the δ^{18}O-Po$_{NaOH}$ was minor, as a difference between the treatments was only observed at day 4, and this subsequently leveled out. The increase in microbial activity observed in the first few weeks after the addition of the litter could have determined a faster turnover of Po derived from microbes. If the microbial Po was isotopically enriched as a consequence of the incorporation of O from labeled water, it would enrich the δ^{18}O-Po$_{NaOH}$ once released from cells. Unfortunately, the δ^{18}O-P of microbial Po is unknown, which prevents the calculation of its contribution to the Po$_{NaOH}$ pool. Measuring the isotopic signature of microbial Po or single microbial metabolites constitutes a major research gap that needs to be investigated in order to better clarify Po dynamics (Tamburini et al., 2018).

CONCLUSION

Until now the isotopic equilibrium between phosphate and water was believed to be the main biological effect on microbial and available P. Here, we show that a below-equilibrium signature can be still an indicator of control of microbial P on the available P via Po hydrolysis reactions. This effect is possibly induced by P limiting conditions for microbes.

Labeling with ^{18}O-water allowed the identification of the major biological process contributing to available P where radioisotope tracers fail because of low sensitivity, i.e., high baseline of isotopic dilution, as in the case of P-rich soils. Two independent isotopic approaches (^{33}P and δ^{18}O-P) provided very similar estimates of P exchanged between the P$_{res}$ and Pi$_{NaOH}$ pools. This suggests that δ^{18}O-P can be successfully used to trace P fluxes, provided that the underlying processes do not break the P – O bonds of the phosphate molecule.

DATA AVAILABILITY STATEMENT

The dataset on fungal and bacterial community composition discussed in this study can be found in the Portail Data INRAE V1 repository (https://doi.org/10.15454/XOFCHY).

AUTHOR CONTRIBUTIONS

CP wrote the manuscript with the inputs from all the co-authors. CP and ÉM conducted the experiments and performed the analyses. EF, FT, EB, and CP contributed to the experiment design. All authors contributed to the article and approved the submitted version.

FUNDING

ACKNOWLEDGMENTS

SUPPLEMENTARY MATERIAL

The Supplementary Material for this article can be found online at: https://www.frontiersin.org/articles/10.3389/fenvs.2020. 564778/full#supplementary-material

REFERENCES

Achat, D. L., Bakker, M. R., Augusto, L., Saur, E., Dousseron, L., Morel, C., et al. (2009). Evaluation of the phosphorus status of P-deficient podzols in temperate pine stands: combining isotopic dilution and extraction methods. *Biogeochemistry* 92, 183–200. doi: 10.1007/s10533-008-9283-7

Alef, K. (1995). "Soil respiration," in *Methods in Soil Microbiology and Biochemistry*, eds K. Alef, and P. Nannipieri (San Diego, CA: Alef K. and Nannipieri P.).

Anderson, G. M. (1976). Error propagation by the Monte Carlo method in geochemical calculations. *Geochim. Cosmochim. Acta* 40, 1533–1538. doi: 10.1016/0016-7037(76)90092-2

Bauke, S. L., Sperber, C., von Siebers, N., Tamburini, F., and Amelung, W. (2017). Biopore effects on phosphorus biogeochemistry in subsoils. *Soil Biol. Biochem.* 111, 157–165. doi: 10.1016/j.soilbio.2017.04.012

Becquer, A., Trap, J., Irshad, U., Ali, M. A., and Claude, P. (2014). From soil to plant, the journey of P through trophic relationships and ectomycorrhizal association. *Front. Plant Sci.* 5:548. doi: 10.3389/fpls.2014.00548

Blagodatskaya, E., and Kuzyakov, Y. (2013). Active microorganisms in soil: critical review of estimation criteria and approaches. *Soil Biol. Biochem.* 67, 192–211. doi: 10.1016/j.soilbio.2013.08.024

Blake, R. E., O'Neil, J. R., and Surkov, A. V. (2005). Biogeochemical cycling of phosphorus: insights from oxygen isotope effects of phosphoenzymes. *Am. J. Sci.* 305, 596–620. doi: 10.2475/ajs.305.6-8.596

Brandtberg, P.-O., Bengtsson, J., and Lundkvist, H. (2004). Distributions of the capacity to take up nutrients by *Betula* spp. and Picea abies in mixed stands. *For. Ecol. Manag.* 198, 193–208. doi: 10.1016/j.foreco.2004.04.012

Buehler, S., Oberson, A., Rao, I. M., Friesen, D. K., and Frossard, E. (2002). Sequential phosphorus Extraction oof a 33P-labeled Oxisol under contrasting agricultural systems. *Soil Sci. Soc. Am. J.* 66, 868–877. doi: 10.2136/sssaj2002.0868

Bünemann, E. K. (2015). Assessment of gross and net mineralization rates of soil organic phosphorus – A review. *Soil Biol. Biochem.* 89, 82–98. doi: 10.1016/j.soilbio.2015.06.026

Bünemann, E. K., Augstburger, S., and Frossard, E. (2016). Dominance of either physicochemical or biological phosphorus cycling processes in temperate forest soils of contrasting phosphate availability. *Soil Biol. Biochem.* 101, 85–95. doi: 10.1016/j.soilbio.2016.07.005

Bünemann, E. K., Steinebrunner, F., Smithson, P. C., Frossard, E., and Oberson, A. (2004). Phosphorus dynamics in a highly weathered soil as revealed by isotopic labeling techniques. *Soil Sci. Soc. Am. J.* 68, 1645–1655. doi: 10.2136/sssaj2004.1645

Chang, S. J., and Blake, R. E. (2015). Precise calibration of equilibrium oxygen isotope fractionations between dissolved phosphate and water from 3 to 37°C. *Geochim. Cosmochim. Acta* 150, 314–329. doi: 10.1016/j.gca.2014.10.030

Chen, J., Seven, J., Zilla, T., Dippold, M. A., Blagodatskaya, E., Kuzyakov, Y., et al. (2019). Microbial C:N:P stoichiometry and turnover depend on nutrients availability in soil: a 14C, 15N and 33P triple labelling study. *Soil Biol. Biochem.* 131, 206–216. doi: 10.1016/j.soilbio.2019.01.017

Cohn, M. (1958). Phosphate-water exchange reaction catalyzed by inorganic pyrophosphatase of yeast. *J. Biol. Chem.* 230, 369–380.

Daroub, S. H., Pierce, F. J., and Ellis, B. G. (2000). Phosphorus fractions and fate of phosphorus-33 in soils under plowing and no-tillage. *Soil Sci. Soc. Am. J.* 64, 170–176. doi: 10.2136/sssaj2000.641170x

Fanin, N., Fromin, N., Buatois, B., and Hättenschwiler, S. (2013). An experimental test of the hypothesis of non-homeostatic consumer stoichiometry in a plant litter–microbe system. *Ecol. Lett.* 16, 764–772. doi: 10.1111/ele.12108

Fardeau, J. C., Guiraud, G., and Marol, C. (1995). The role of isotopic techniques on the evaluation of the agronomic effectiveness of P fertilizers. *Nutr. Cycling Agroecosyst.* 45, 101–109. doi: 10.1007/bf00790659

Frossard, E., Achat, D. L., Bernasconi, S. M., Bünemann, E. K., Fardeau, J.-C., Jansa, J., et al. (2011*). "The use of tracers to investigate phosphate cycling in soil–plant systems," in *Phosphorus in Action*. (Berlin: Bunemann E. K.).

Gross, A., and Angert, A. (2015). What processes control the oxygen isotopes of soil bio-available phosphate? *Geochim. Cosmochim. Acta* 159, 100–111.

Gross, A., and Angert, A. (2017). Use of 13 C- and phosphate 18 O-labeled substrate for studying phosphorus and carbon cycling in soils: a proof of concept: 13 C- and P- 18 O dual-labeled substrate to trace soil C and P cycling. *Rapid Commun. Mass Spectrom.* 31, 969–977. doi: 10.1002/rcm.7863

Hauenstein, S., Neidhardt, H., Lang, F., Krüger, J., Hofmann, D., Pütz, T., et al. (2018). Organic layers favor phosphorus storage and uptake by young beech trees (*Fagus sylvatica* L.) at nutrient poor ecosystems. *Plant Soil* 432, 289–301. doi: 10.1007/s11104-018-3804-5

Helfenstein, J., Pistocchi, C., Oberson, A., Tamburini, F., Goll, D. S., Frossard, E., et al. (2020). Estimates of mean residence times of phosphorus in commonly considered inorganic soil phosphorus pools. *Biogeosciences* 17, 441–454. doi: 10.5194/bg-17-441-2020

Helfenstein, J., Tamburini, F., von Sperber, C., Massey, M. S., Pistocchi, C., Chadwick, O. A., et al. (2018). Combining spectroscopic and isotopic techniques gives a dynamic view of phosphorus cycling in soil. *Nat. Commun.* 9:3226.

IUSS Working Group WRB (2006). *World Reference Base for Soil Resources 2006 – A Framework for International Classification, Correlation and Communication*. Rome: Food and Agriculture Organization of the United Nations.

Jaisi, D. P., Blake, R. E., and Kukkadapu, R. K. (2010). Fractionation of oxygen isotopes in phosphate during its interactions with iron oxides. *Geochim. Cosmochim. Acta* 74, 1309–1319. doi: 10.1016/j.gca.2009.11.010

Jonard, M., Augusto, L., Morel, C., Achat, D. L., and Saur, E. (2009). Forest floor contribution to phosphorus nutrition: experimental data. *Ann. For. Sci.* 66:510. doi: 10.1051/forest/2009039

Kottur, J., and Nair, D. T. (2018). Pyrophosphate hydrolysis is an intrinsic and critical step of the DNA synthesis reaction. *Nucleic Acids Res.* 46, 5875–5885. doi: 10.1093/nar/gky402

Kouno, K., Tuchiya, Y., and Ando, T. (1995). Measurement of soil microbial biomass phosphorus by an anion exchange membrane method. *Soil Biol. Biochem.* 27, 1353–1357. doi: 10.1016/0038-0717(95)00057-l

Lang, F., Krüger, J., Amelung, W., Willbold, S., Frossard, E., Bünemann, E. K., et al. (2017). Soil phosphorus supply controls P nutrition strategies of beech forest ecosystems in Central Europe. *Biogeochemistry* 136, 5–29. doi: 10.1007/s10533-017-0375-0

Liang, Y., and Blake, R. E. (2006a). Oxygen isotope composition of phosphate in organic compounds: isotope effects of extraction methods. *Organic Geochem.* 37, 1263–1277. doi: 10.1016/j.orggeochem.2006.03.009

Liang, Y., and Blake, R. E. (2006b). Oxygen isotope signature of Pi regeneration from organic compounds by phosphomonoesterases and photooxidation. *Geochim Cosmochim. Acta* 70, 3957–3969. doi: 10.1016/j.gca.2006.04.036

Lis, H., Weiner, T., Pitt, F. D., Keren, N., and Angert, A. (2019). Phosphate Uptake by Cyanobacteria Is Associated with Kinetic Fractionation of Phosphate Oxygen Isotopes. *ACS Earth Space Chem.* 3, 233–239. doi: 10.1021/acsearthspacechem.8b00099

Longinelli, A., and Nuti, S. (1973). Revised phosphate-water isotopic temperature scale. *Earth Planet. Sci. Lett.* 19, 373–376. doi: 10.1016/0012-821x(73)90088-5

Manzoni, S., Trofymow, J. A., Jackson, R. B., and Porporato, A. (2010). Stoichiometric controls on carbon, nitrogen, and phosphorus dynamics in decomposing litter. *Ecol. Monogr.* 80, 89–106. doi: 10.1890/09-0179.1

Marx, M.-C., Wood, M., and Jarvis, S. C. (2001). A microplate fluorimetric assay for the study of enzyme diversity in soils. *Soil Biol. Biochem.* 33, 1633–1640. doi: 10.1016/s0038-0717(01)00079-7

Melby, E. S., Soldat, D. J., and Barak, P. (2013). Biological decay of 18O-labeled phosphate in soils. *Soil Biol. Biochem.* 63, 124–128. doi: 10.1016/j.soilbio.2013.03.020

Mészáros, É., Pistocchi, C., Frossard, E., Buenemann, E. K., and Tamburini, F. (2020*). Changes of fungal and bacterial community composition of forest organic horizons with low and high phosphorus availability, Portail Data INRAE, V1. doi: 10.15454/XOFCHY

Mooshammer, M., Wanek, W., Schnecker, J., Wild, B., Leitner, S., Hofhansl, F., et al. (2012). Stoichiometric controls of nitrogen and phosphorus cycling in decomposing beech leaf litter. *Ecology* 93, 770–782.

Mooshammer, M., Wanek, W., Zechmeister-Boltenstern, S., and Richter, A. (2014). Stoichiometric imbalances between terrestrial decomposer communities and their resources: mechanisms and implications of microbial adaptations to their resources. *Front. Microbiol.* 5:22. doi: 10.3389/fmicb.2014.00022

Noack, S. R., Smernik, R. J., McBeath, T. M., Armstrong, R. D., and McLaughlin, M. J. (2014). Assessing crop residue phosphorus speciation using chemical fractionation and solution 31P nuclear magnetic resonance spectroscopy. *Talanta* 126, 122–129. doi: 10.1016/j.talanta.2014.03.049

Oehl, F., Oberson, A., Sinaj, S., and Frossard, E. (2001). Organic phosphorus mineralization studies using isotopic dilution techniques. *Soil Sci. Soc. Am. J.* 65, 780–787. doi: 10.2136/sssaj2001.653780x

Ohno, T., and Zibilske, L. (1991). Determination of low concentrations of phosphorus in soil extracts using malachite green. *Soil Sci. Soc. Am. J.* 55, 892–895. doi: 10.2136/sssaj1991.03615995005500030046x

Orlowski, N., Frede, H. G., Brüggemann, N., and Breuer, L. (2013). Validation and application of a cryogenic vacuum extraction system for soil and plant water extraction for isotope analysis. *J Sensors Sensor Syst.* 2, 179–193. doi: 10.5194/jsss-2-179-2013

Pfahler, V., Dürr-Auster, T., Tamburini, F., Bernasconi, S. M., and Frossard, E. (2013). 18 O enrichment in phosphorus pools extracted from soybean leaves. *New Phytol.* 197, 186–193. doi: 10.1111/j.1469-8137.2012.04379.x

Pistocchi, C., Mészáros, É, Tamburini, F., Frossard, E., and Bünemann, E. K. (2018). Biological processes dominate phosphorus dynamics under low phosphorus availability in organic horizons of temperate forest soils. *Soil Biol. Biochem.* 126, 64–75.

Pistocchi, C., Tamburini, F., Gruau, G., Ferhi, A., Trevisan, D., Dorioz, J. M., et al. (2017). Tracing the sources and cycling of phosphorus in river sediments using oxygen isotopes: methodological adaptations and first results from a case study in France. *Water Res.* 111, 346–356.

Pistocchi, C., Tamburini, F., Savoye, L., Sebilo, M., Baneschi, L., Lacroix, D., et al. (2014*). Développement d'une méthode d'extraction et purification des phosphates à partir de matrices sédimentaires pour l'analyse isotopique de leur oxygène. *Le cahier des techniques de l'INRA* 81, 1–23.

Poll, C., Ingwersen, J., Stemmer, M., Gerzabek, H., and Kandeler, E. (2006). Mechanisms of solute transport affect small-scale abundance and function of soil microorganisms in the detritusphere. *Eur. J. Soil Sci.* 57, 583–595. doi: 10.1111/j.1365-2389.2006.00835.x

Saaby Johansen, H., Middelboe, V., and Larsen, S. (1991). *Delabelling of 18O Enriched Phosphate Added to Soil as a Function of Biological Activity in the Soil.* Vienna: IAEA.

Seth, B., Schneider, C., and Storck, F. (2006). Improved reliability of oxygen isotopic analysis of water using the Finnigan GasBench II periphery of a continuous flow isotope ratio mass spectrometer by backflushing of the sampling line. *Rapid Commun. Mass Spectrom.* 20, 1049–1051. doi: 10.1111/j.1365-2389.2006.00835.x

Siebers, N., Bauke, S. L., Tamburini, F., and Amelung, W. (2018). Short-term impacts of forest clear-cut on P accessibility in soil microaggregates: an oxygen isotope study. *Geoderma* 315, 59–64. doi: 10.1016/j.geoderma.2017.11.024

Siegenthaler, M. B., Tamburini, F., Frossard, E., Chadwick, O. A., Vitousek, P., Chiara, P., et al. (2020). A dual isotopic (32P and 18O) incubation study to disentangle mechanisms controlling phosphorus cycling in soils from a climatic gradient (Kohala, Hawaii). *Soil Biol. Biochem.* 149:107920. doi: 10.1016/j.soilbio.2020.107920

Spohn, M., and Chodak, M. (2015). Microbial respiration per unit biomass increases with carbon-to-nutrient ratios in forest soils. *Soil Biol. Biochem.* 81, 128–133. doi: 10.1016/j.soilbio.2014.11.008

Spohn, M., Ermak, A., and Kuzyakov, Y. (2013). Microbial gross organic phosphorus mineralization can be stimulated by root exudates – A 33P isotopic dilution study. *Soil Biol. Biochem.* 65, 254–263. doi: 10.1016/j.soilbio.2013.05.028

Stout, L. M., Joshi, S. R., Kana, T. M., and Jaisi, D. P. (2014). Microbial activities and phosphorus cycling: an application of oxygen isotope ratios in phosphate. *Geochim. Cosmochim. Acta* 138, 101–116. doi: 10.1016/j.gca.2014.04.020

Tamburini, F., Bernasconi, S. M., Angert, A., and Frossard, E. (2010). A method for the analysis of the δ18O of inorganic phosphate extracted from soils with HCl. *Eur. J. Soil Sci.* 61, 1025–1032. doi: 10.1111/j.1365-2389.2010.01290.x

Tamburini, F., Pfahler, V., Bünemann, E. K., Guelland, K., Bernascon, S. M., Frossard, E., et al. (2012). Oxygen isotopes unravel the role of microorganisms in phosphate cycling in soils. *Environ. Sci. Technol.* 46, 5956–5962. doi: 10.1021/es300311h

Tamburini, F., Pistocchi, C., Helfenstein, J., and Frossard, E. (2018). A method to analyse the isotopic composition of oxygen associated with organic phosphorus in soil and plant material. *Eur. J. Soil Sci.* 69, 816–826. doi: 10.1111/ejss.12693

Tiessen, H., and Moir, J. O. (1993). "Characterization of Available P by Sequential Extraction," in *Soil Sampling and Methods of Analysis*, eds M. R. Carter, and E. G. Gregorich (Ann Arbor, MI: Carter M.R).

Tudge, A. P. (1960). A method of analysis of oxygen isotopes in orthophosphate—its use in the measurement of paleotemperatures. *Geochim. Cosmochim. Acta* 18, 81–93. doi: 10.1016/0016-7037(60)90019-3

von Sperber, C., Kries, H., Tamburini, F., Bernasconi, S. M., and Frossard, E. (2014). The effect of phosphomonoesterases on the oxygen isotope composition of phosphate. *Geochim. Cosmochim. Acta* 125, 519–527. doi: 10.1016/j.gca.2013.10.010

von Sperber, C., Tamburini, F., Brunner, B., Bernasconi, S. M., and Frossard, E. (2015). The oxygen isotope composition of phosphate released from phytic acid by the activity of wheat and Aspergillus niger phytase. *Biogeosciences* 12, 4175–4184. doi: 10.5194/bg-12-4175-2015

Weiner, T., Gross, A., Moreno, G., Migliavacca, M., Schrumpf, M., Reichstein, M., et al. (2018). Following the turnover of soil bioavailable phosphate in mediterranean savanna by oxygen stable isotopes. *J. Geophys. Res.* 123, 1850–1862. doi: 10.1029/2017JG004086

Werner, F., Mueller, C. W., Thieme, J., Gianoncelli, A., Rivard, C., Höschen, C., et al. (2017). Micro-scale heterogeneity of soil phosphorus depends on soil substrate and depth. *Sci. Rep.* 7:3203. doi: 10.1038/s41598-017-03537-8

Zohar, I., Shaviv, A., Young, M., Kendall, C., Silva, S., Paytan, A., et al. (2010). Phosphorus dynamics in soils irrigated with reclaimed waste water or fresh water — A study using oxygen isotopic composition of phosphate. *Geoderma* 159, 109–121. doi: 10.1016/j.geoderma.2010.07.002